

Aberystwyth University

Spatial analysis of early mangrove regeneration in the Matang Mangrove Forest Reserve, Peninsular Malaysia, using geomatics

Otero, Viviana; Lucas, Richard; Van De Kerchove, Ruben; Satyanarayana, Behara; Mohd-Lokman, Husain; Dahdouh-Guebas, Farid

Published in:
Forest Ecology and Management

DOI:
[10.1016/j.foreco.2020.118213](https://doi.org/10.1016/j.foreco.2020.118213)

Publication date:
2020

Citation for published version (APA):
Otero, V., Lucas, R., Van De Kerchove, R., Satyanarayana, B., Mohd-Lokman, H., & Dahdouh-Guebas, F. (2020). Spatial analysis of early mangrove regeneration in the Matang Mangrove Forest Reserve, Peninsular Malaysia, using geomatics. *Forest Ecology and Management*, 472, [118213].
<https://doi.org/10.1016/j.foreco.2020.118213>

General rights

Copyright and moral rights for the publications made accessible in the Aberystwyth Research Portal (the Institutional Repository) are retained by the authors and/or other copyright owners and it is a condition of accessing publications that users recognise and abide by the legal requirements associated with these rights.

- Users may download and print one copy of any publication from the Aberystwyth Research Portal for the purpose of private study or research.
- You may not further distribute the material or use it for any profit-making activity or commercial gain
- You may freely distribute the URL identifying the publication in the Aberystwyth Research Portal

Take down policy

If you believe that this document breaches copyright please contact us providing details, and we will remove access to the work immediately and investigate your claim.

tel: +44 1970 62 2400
email: is@aber.ac.uk

Spatial analysis of early mangrove regeneration in the Matang Mangrove Forest Reserve, peninsular Malaysia

Viviana Otero^{1§}, Richard Lucas^{2,3}, Ruben Van De Kerchove⁴, Behara Satyanarayana⁵, Mohd Lokman Bin Husain⁵, Farid Dahdouh-Guebas^{1,6}

1 Systems Ecology & Resource Management Laboratory, Université Libre de Bruxelles (ULB), Brussels, Belgium

2 Earth Observation and Ecosystem Dynamics Research Group, Aberystwyth University, Aberystwyth, UK

3 School of Biological, Earth and Environmental Sciences, University of New South Wales (UNSW), Sydney, Australia

4 Vlaamse Instelling Voor Technologisch Onderzoek (VITO) Research Organisation, Mol, Belgium

5 Mangrove Research Unit, Institute of Oceanography and Environment, Universiti Malaysia Terengganu (UMT), Kuala Terengganu, Malaysia

6 Laboratory of Plant Biology and Nature Management, Vrije Universiteit Brussel (VUB), Brussels, Belgium

§ Corresponding author at: Avenue F.D. Roosevelt 50, CPI 264/1, B-1050 Bruxelles, Belgium. Email address: voterofa@ulb.ac.be

Abstract

Successful mangrove tree regeneration is required to maintain the provision of wood for silviculturally managed mangrove forest areas and to ensure mangrove rehabilitation in disturbed areas. Successful natural regeneration of mangroves after disturbance depends on the dispersal, establishment, early growth and survival of propagules. Focusing on the Matang Mangrove Forest Reserve (MMFR) in Peninsular Malaysia,

we investigated how the location of a mangrove forest patch might influence the early regeneration of mangroves after clear-felling events that regularly take place on an approximately 30 year rotation as part of local management. We used Landsat-derived Normalized Difference Moisture Index (NDMI) annual time series from 1988 to 2015 to indicate the recovery of canopy cover during early regeneration, which was determined as the average time (in years) for the NDMI to recover to values associated with the mature forests prior to their clear felling. We found that clear-felled mangrove patches closer to water and/or to already established patches of *Rhizophora* regenerated more rapidly than those that were found farther away. The study concludes that knowledge of the distribution of water (and particularly hydro-period) and vegetation communities across the landscape can indicate the likely regeneration of mangrove forests through natural processes and identify areas where active planting is needed. Furthermore, time-series comparisons of the NDMI during the early years of regeneration can assist monitoring of mangrove establishment and regeneration, inform on the success of replanting, and facilitate higher productivity within the MMFR.

Keywords: mangroves, mangrove regeneration, silviculture, spatial analysis

Abbreviations

GLS	Generalized Least Squares
MMFR	Matang Mangrove Forest Reserve
NDMI	Normalized Difference Moisture Index
NDVI	Normalized Difference Vegetation Index
SD	Standard Deviation
SPOT	Satellite Pour l'Observation de la Terre
UTM	Universal Transverse Mercator

1. Introduction

Provision of wood for timber and poles has been a traditional use of mangrove ecosystems (Alongi, 2002, Walters *et al.*, 2008, Saenger, 2002). Silviculture, among others, has been one of the primary drivers of mangrove restoration projects (Bosire *et al.*, 2008, Ellison, 2000, Lopez-Portillo *et al.*, 2017). Successful mangrove tree regeneration is required to ensure a sustainable silvicultural management in order to maintain the provision of wood.

Successful natural regeneration of mangroves after a disturbance depends on the dispersal, establishment, early growth and survival of propagules and seedlings (Di Nitto *et al.*, 2013, Sillanpaa *et al.*, 2017, Tomlinson, 2016). Propagule dispersal requires a normal tidal flooding and sufficient propagules in adjacent mangrove stands (Bosire *et al.*, 2008, Kairo *et al.*, 2001, Lewis III, 2005) and, as with establishment, are affected by factors such as wind speed, freshwater discharge, geomorphology, trapping agents, propagule morphology, propagule predation, light and nutrient availability (Di Nitto *et al.*, 2013, Komiyama *et al.*, 1996, Sousa *et al.*, 2007; Tomlinson, 2016, Van der Stocken *et al.*, 2015, Van Nederveelde *et al.*, 2015).

Spatial information on the extent, state and dynamics of coastal environments is important for understanding the recovery of mangroves following a disturbance (Rivera-Monroy *et al.*, 2004) and other biological processes (Hickey *et al.*, 2018, Kock *et al.*, 2009, Ribeiro *et al.*, 2009). Remote sensing data can provide such information over varying (sub-annual to multi-decadal) spatial and temporal scales (Cammaretta *et al.*, 2018, Herold *et al.*, 2005, Hickey *et al.*, 2018). As such, these data have been used for land cover classification, species mapping, biomass, landscape metrics calculation and disturbance detection (*e.g.* Amir, 2012, Aslan *et al.*, 2016, Bunting *et al.*, 2018, Conchedda *et al.*, 2008, Hamunyela *et al.*, 2016, Hickey *et al.*, 2018, Simard *et al.*, 2019, Suyadi *et al.*, 2018). However, few studies have used spatial information extracted from remote sensing to study spatial trends in mangrove regeneration (Suyadi *et al.*, 2018, Hickey *et al.*, 2018), although there have been many field-based studies (*e.g.* Kairo *et al.*,

2001, Lewis III, 2005, Peng *et al.*, 2016, Putz and Chan, 1986, Sillanpaa *et al.*, 2017, Sousa *et al.*, 2003; Sousa *et al.*, 2007; Tomlinson, 2016).

Focusing on the Matang Mangrove Forest Reserve (MMFR) in Peninsular Malaysia, this study aimed to establish whether forest regeneration rates varied within and between forest patches that were clear felled and, if so, whether recovery varied as a function of proximity to the cleared area, other mangrove forests (as a function of their species dominance), terrestrial (dryland) forests or water. Aziz *et al.* (2015, 2016) identified that some areas in the MMFR experienced different regeneration rates, which can impact the greenwood yield and carbon sequestration in the reserve. Although, mangrove regeneration at MMFR has been studied using ground-based forest inventories (*e.g.* Amir, 2012, Goessens *et al.*, 2014, Gong and Ong, 1995, Putz and Chan, 1986), the use of remote sensing data and the relationship between regeneration and proximity to other types of land cover has also not been studied.

2. Materials and Methods

2.1 Study area

The MMFR has been under management since 1902 (Chong, 2006). The reserve is a riverine mangrove forest of 27 different true mangrove species and provides ecosystem services such as wood provision for charcoal and pole production, coastal protection, conservation of flora and fauna, ecotourism, fishery maintenance and mangrove propagule production (Ariffin and Mustafa, 2013). The MMFR occupies an area of 40,288 ha and has a tropical climate with an average air temperature ranging from 22°C to 33°C (Ariffin and Mustafa, 2013). The rainfall rate is between 2,000 mm and 2,800 mm per year (Ariffin and Mustafa, 2013). Tides are semidiurnal with an amplitude of 3.3 m (Ashton *et al.*, 1999). Medium height tides (2.4 to 3.4 m height above chart datum) inundate *Rhizophora* stands that are near the tidal creeks (Ariffin and Mustafa, 2013). Normal height tides (3.4 to 4 m height above chart datum) inundate extensive central mangrove areas that are normally composed by *Rhizophora apiculata* Blume and *Bruguiera* mangrove trees (Ariffin and Mustafa, 2013).

The MMFR is divided into four different types of administrative zones: protective (17.4% of the total forest area in the Reserve), productive (74.8%), restrictive productive (6.8%) and unproductive (1%) (Figure 1a) (Ariffin and Mustafa, 2013). The productive and restrictive productive zones are exploited for timber extraction to produce charcoal and poles. These zones are composed of forests dominated primarily by *R. apiculata* and *R. mucronata* Lamk. The current silvicultural management consists of a 30 year rotation cycle with two thinnings at 15 and 20 years (Ariffin and Mustafa, 2013, Chong, 2006). The protective zones are not intended to provide wood for charcoal and pole production. The unproductive zones are lakes and infrastructure areas, including urban villages, charcoal kilns and offices (Ariffin and Mustafa, 2013).

The protective zones are composed of different mangrove formation communities (Ariffin and Mustafa, 2013): (i) *Avicennia-Sonneratia* stands, (ii) *Rhizophora* stands and (iii) the dryland forest stands (Figure 1b). (i) The *Avicennia-Sonneratia* stands are typically composed of young stands of *Avicennia* trees that are colonising the new mudflats. The dominant species in these stands are *Avicennia alba* Blume and *A. officinalis* L., although it is also possible to find patches of *Sonneratia alba* J. Smith within the clusters of *A. alba* and *A. officinalis*. These stands are inundated by all high tides (0 to 2.4 m height above chart datum) (*loc.cit.*). The size of these stands is 3,299 ha (*loc.cit.*). (ii) The *Rhizophora* stands within the protective zone are formations of *R. apiculata* and *R. mucronata* that are not under exploitation. *R. apiculata* is the dominant species and *R. mucronata* is usually found along the banks of the tidal creeks and streams (*loc.cit.*). The size of these stands is 1,665 ha (iii) The dryland forest stands are the transition to inland forest. These stands are characterised by the predominance of dense patches of *Acrostichum aureum* L. on the forest floor with scattered pockets of dryland trees (Ariffin and Mustafa, 2013).

Dryland forests stands are composed of 30 different tree species (Chan, 1989). Four out of the 30 tree species are major and minor elements of mangroves according to Tomlinson (2016) (see supplementary data Table S1). The dryland forest stands are inundated by equinoctial tides (4 to 4.6 m height above chart

datum) and are found in more elevated areas in the landward side. The dryland forest stands size is 2,291 ha (Ariffin and Mustafa, 2013).

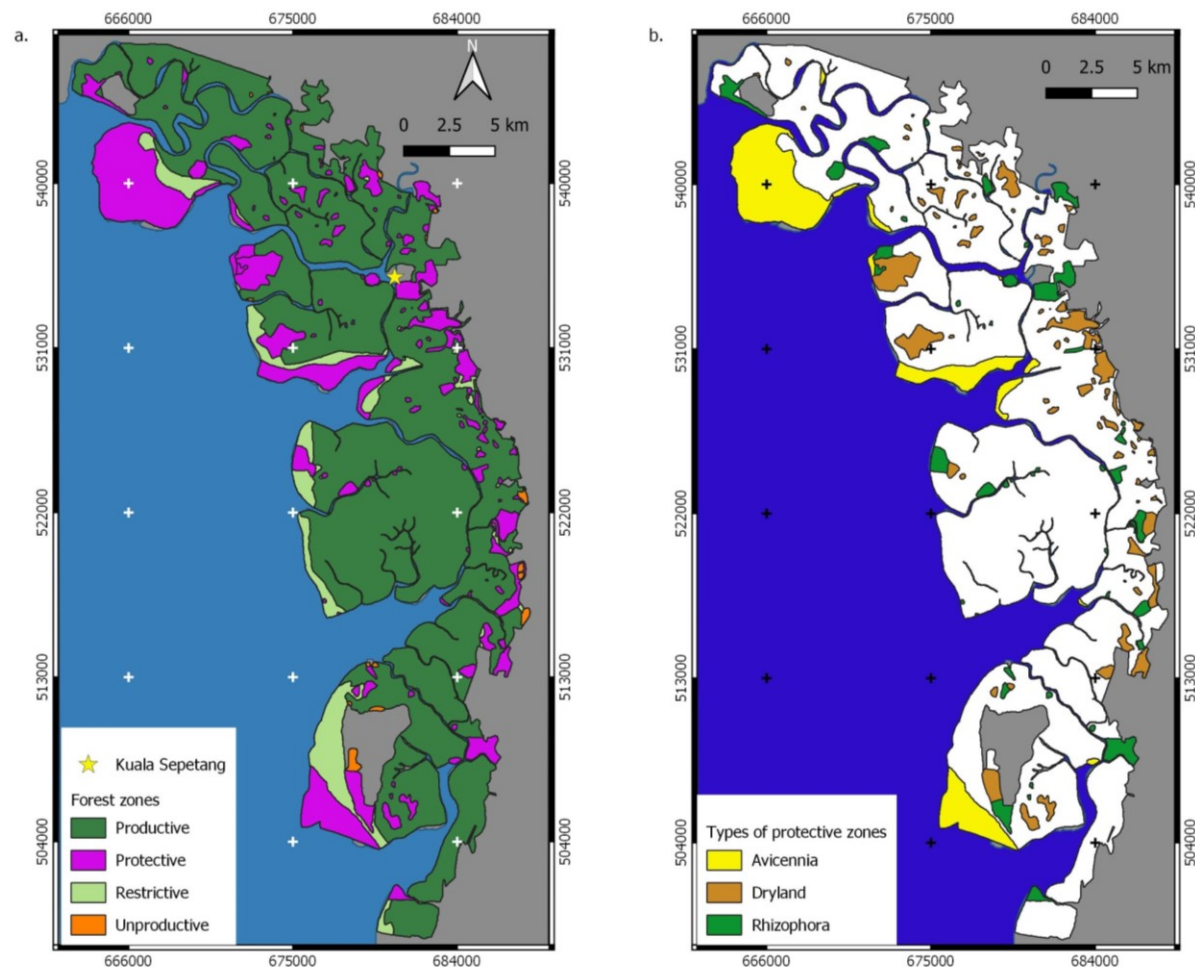


Figure 1. a) The management zones of the MMFR on the west coast of Peninsular Malaysia (based on Ariffin and Mustafa, 2013, Otero *et al.*, 2019), with these referred to as productive, restrictive productive, protective and unproductive zones (Taken from Otero *et al.*, 2019). The species composition of each zone differs, with the productive and restrictive productive zones comprised primarily of *R. apiculata* and *R. mucronata* species. The protective zones are more diverse in terms of mangrove species composition. Within the protective zones, the main types of forest occurring are *Avicennia-Sonneratia* stands, *Rhizophora* stands and the dryland forest stands (Figure 1b). The grey areas represent areas outside of the reserve.

The management plan of the reserve is defined every ten years and includes the planning of the thinning and clear-felling activities. The clear-felling activities are performed by approved charcoal contractors, who can choose the areas that they are going to harvest according to an order pre-defined via balloting (Ariffin and Mustafa, 2013, p. 48). The assignment of the areas to be clear-felled by certain contractors are included in the management plan as are maps that indicate the year when certain areas are planned to be cut. Each contractor receives an area between 2.2 ha and 6.6 ha to clearfell and extract wood to produce charcoal (Ariffin and Mustafa, 2013). The contractors are obliged to fell both the commercial (*R. apiculata* and *R. mucronata*) and non-commercial species (*Bruguiera parviflora* Wight & Arnold ex Griffith and *Bruguiera cylindrica* (Linnaeus) Blume). In addition, the Forestry Department is in charge of weeding operations in recently clear-felled areas that have been colonized by *Acrostichum* ferns (Ariffin and Mustafa, 2013, p. 58).

The management implements a policy of active replanting, which is performed by qualified contractors who source and plant propagules (Ariffin and Mustafa, 2013, p. 53). The traditional method for replanting is to plant propagules directly. Planting using seedlings grown in plastic bags is used for problematic areas (e.g. those that are deeply flooded, contain significant populations of crabs and monkeys, or are contained within the restrictive productive zones) (Ariffin and Mustafa, 2013, p. 53). The decision on where to replant is based on the assessment of all clear-felled areas two years after a clear-felling event. If the natural regeneration is less than 90 %, *Rhizophora* propagules or seedlings (for problematic areas) are planted where needed (Ariffin and Mustafa, 2013, p. 55). Although this is the reported strategy, we were informed that the current reference for replanting is 70 % instead of 90 % (March 2019 by personal communication with a local officer). *Rhizophora apiculata* propagules are planted at a spacing of 1.2 m x 1.2 m, and *Rhizophora mucronata* propagules are planted at a spacing of 1.8 m x 1.8 m (Ariffin and Mustafa, 2013, p. 55).

2.2 Mangrove regeneration

In this study, we focus on the period of regeneration between the clearing event and the attainment of an areal canopy cover that is broadly equivalent to that associated with the mature forests prior to clearing. On this basis, we quantify the early recovery based on the Normalized Difference Moisture Index (NDMI) time series (Otero *et al.*, 2019), as this has been shown to be indicative of percentage canopy cover (Lucas *et al.*, 2019). This recovery time was defined as the number of years that the NDMI recovered to values observed prior to the clear-felling event. Therefore, only the first years of mangrove regeneration are quantified as the NDMI vegetation index saturates in dense vegetation (see Otero *et al.*, 2019 for more details).

Additionally, the map that contained the information of the year of clear felling (from Otero *et al.*, 2019) was used to define the extent of the coupes, with each representing an area of mangrove forest that was clear felled in the same year. The recovery time was considered for each 30 m pixel associated with the Landsat sensor data and associated NDMI time series (Otero *et al.*, 2019).

2.3 Distances calculation

For each coupe defined using a pre-determined clear-felling map (Otero *et al.*, 2019), the centre of each coupe was calculated using the *Centroids* tool available in QGIS (QGIS Development Team, 2018). Afterwards, for each centre, the following information was extracted (Figure 2):

- a. The coordinates of the centre projected in the Universal Transverse Mercator (UTM) Zone 47N, with each assigned with a unique ID
- b. The primary year of clear-felling for each coupe, based on Otero *et al.* (2019), noting that some coupes mapped in the management plan can be cleared over 2 or more years (Lucas *et al.*, 2019) and hence the area of coupes created in a year may differ from that in the management plan.

- c. The average and standard deviation of recovery time based on all the pixels within each identified coupe. This recovery time was defined as the number of years that the NDMI recovered to values observed prior to the clear-felling event (Otero *et al.*, 2019).
- d. The straight line distance to the closest water body (*i.e.*, sea, tidal creeks) based on a water mask, which was created from Landsat sensor data from 1988 to 2015 with the Normalized Difference Vegetation Index (NDVI) time series (from Otero *et al.*, 2019).
- e. The distance to the closest *Rhizophora* stand, which was determined from two existing maps: (i) the management plan map that describes the protective zones and indicates the location of *Rhizophora* stands in these zones (green areas in Figure 1b), and (ii) the management plan map that describes the productive and restrictive productive forests that are mainly composed of *Rhizophora* species (Figure 1a). We combined the previous two maps in a single map that contained the areas where *Rhizophora* stands were considered to be present, noting that some changes or differences might have occurred since their production and/or because of errors in mapping respectively. Afterwards, we removed the areas that were clear-felled between 1989 and 2015 based on the clear-felling map created by Otero *et al.* (2019). The result was a layer that contains the *Rhizophora* stands of the reserve that were not clear-felled between 1989 and 2015.
- f. The distance to the closest dryland forest stand within the protective zones based on the management plan map that describes the protective zones (Figure 1b). All the distance variables were calculated using the *v.distance* tool from GRASS available in QGIS (QGIS Development Team, 2018).

We used the centres of each coupe as a proxy for its location, thereby minimizing border effects. Additionally, we found cases where the distance from a coupe centre to a *Rhizophora* stand or to dryland forest stands was zero and we removed these cases from further analyses (3 % of the cases in total). These cases were 1.3 % of all the centres for the distances to *Rhizophora* stands and 1.6 % for the distances to dryland forest stands. In the case of the *Rhizophora* forests, the centre of the coupe was outside the

corresponding coupe because the original coupe had an irregular shape and the centre was located inside another *Rhizophora* stand. In the cases for the dryland forest stands, we found coupes that were clear-felled in areas that, according to the management plan, are protective zones comprised of dryland forests.

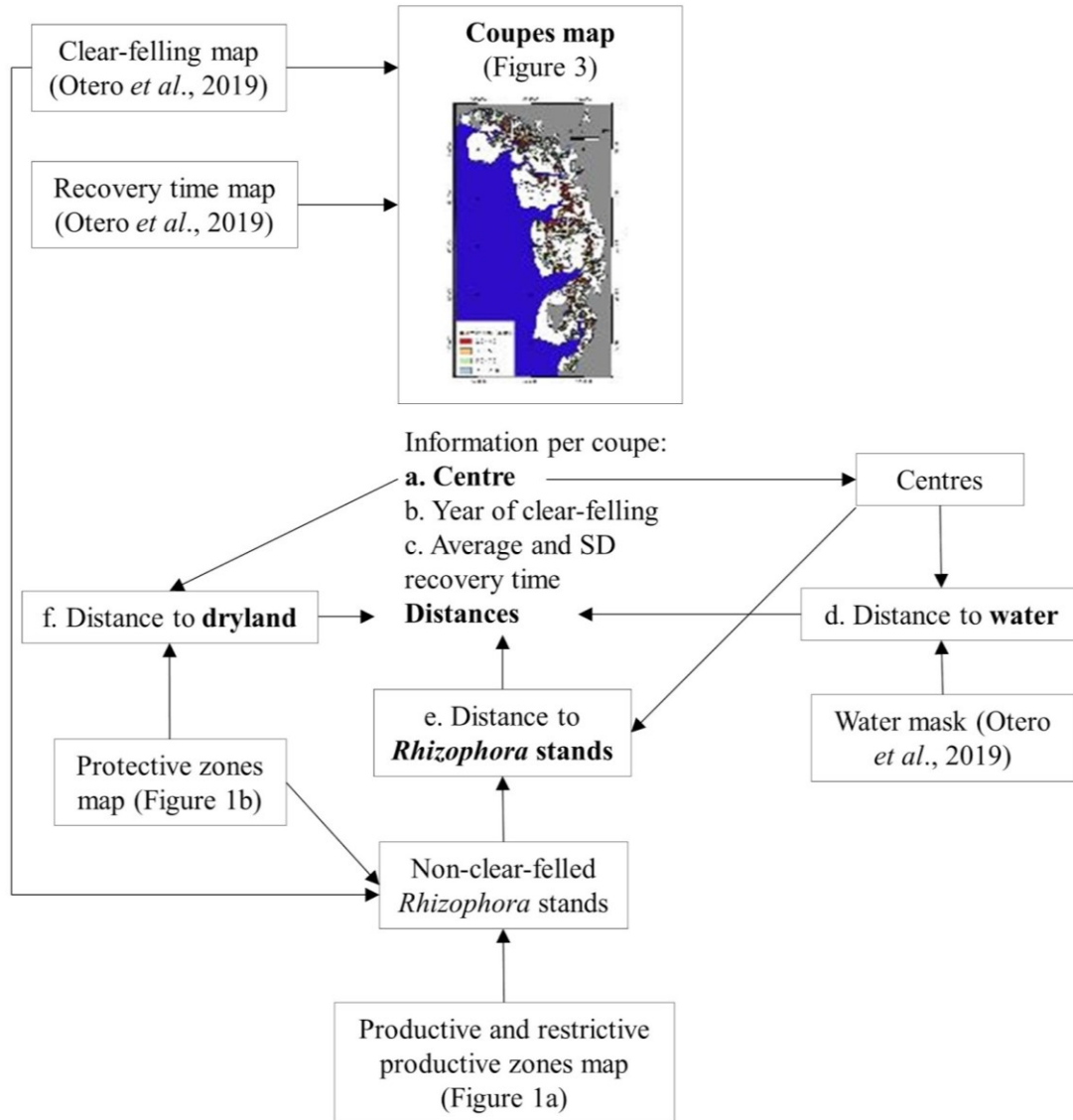


Figure 2. Workflow followed to calculate the attributes of each coupe. The clear-felling map, the recovery time map and the water mask were taken from Otero *et al.* (2019). The local management maps that contain the location of the productive, restrictive productive, protective and unproductive zones, and the types of forests within the protective zones were digitized using the printed maps available in Ariffin and Mustafa (2013). The distance measures used the location of the centre of each coupe, calculated using the *Centroids* tool available in QGIS. The distances to the

different types of land cover were calculated using the *v.distance* GRASS tool available in QGIS. The average and the standard deviation (SD) were calculated using the summary statistics tool available in QGIS. The letters correspond to the previous paragraphs.

2.4 Spatial context analysis

2.4.1 Univariate analysis

We calculated four quartiles (25 %, 50 %, 75 % and 100 %) of the **(i) average** and **(ii) standard deviation** of the **recovery time** per coupe. We compared the distribution of these four quartiles for each of the distances calculated: to water, *Rhizophora* stands, and dryland forest stands. Medians of each quartile group of the recovery time were compared using the Wilcoxon Rank test because each quartile did not have a normal distribution (Shapiro-Wilk test, $p\text{-value}<0.0001$) for the average and standard deviation groups. These analyses were performed in RStudio version 1.1.456, R version 3.6.1 (RStudio Team, 2016).

We repeated the previous analyses by grouping quartiles of similar average time and standard deviation of the recovery time. We grouped the first, second and third quartiles (*i.e.* 25 %, 50 % and 75 %) into one group. A second group was defined that corresponded to the fourth quartile (highest 25 % values). Medians of each quartile group of the recovery time were compared using the Wilcoxon Rank test. We used this statistical test because the distribution of each group did not have a normal distribution (Shapiro-Wilk test, $p\text{-value}<0.0001$).

2.4.2 Multivariate analysis

We used Generalized Least Squares (GLS) models to evaluate the influence of the different types of land cover in the recovery time. We tested the influence of the distance to water bodies, dryland forest stands and remaining *Rhizophora* stands in the average and standard deviation of the recovery time per coupe using two models (Equation 1 and 2):

$$(i) \text{ Average Recovery time} = f(\text{distance to water, distance to dryland forest stands, distance to } Rhizophora \text{ stands}) \quad \text{Equation 1}$$

$$(ii) \text{ Standard deviation Recovery time} = f(\text{distance to water, distance to dryland forest stands, distance to } Rhizophora \text{ stands}) \quad \text{Equation 2}$$

Both models were corrected for spatial autocorrelation by using a Gaussian structure in each one. Additionally, the Nagelkerke adjusted R^2 was reported for each model (Magee, 1990, Nagelkerke, 1991). These statistical analyses were performed in RStudio version 1.1.456, R version 3.6.1, using the *stats*, *nlme* and *rcompanion* packages (RStudio Team, 2016).

3. Results

3.1 Distance calculation

The spatial distribution of forests that were cleared in the same year (and hence identified as coupes) and their associated recover times based on the NDMI time-series is shown in Figure 3. Only the coupes that recovered by 2015 are included in this study (*i.e.* 3,127 coupes). In total, 10,943 ha were clear-felled and for each coupe, the NDMI recovered to the values observed prior to clearing. The average recovery time taking into account all the coupes (by 2015) was 5.6 ± 2.4 years. The median recovery time (interquartile range) was 5 years (4 - 7 years). The minimum recovery time was 2 years and the maximum was 23 years. Only two coupes had a recovery time of 23 years, which correspond to 0.36 ha in total.

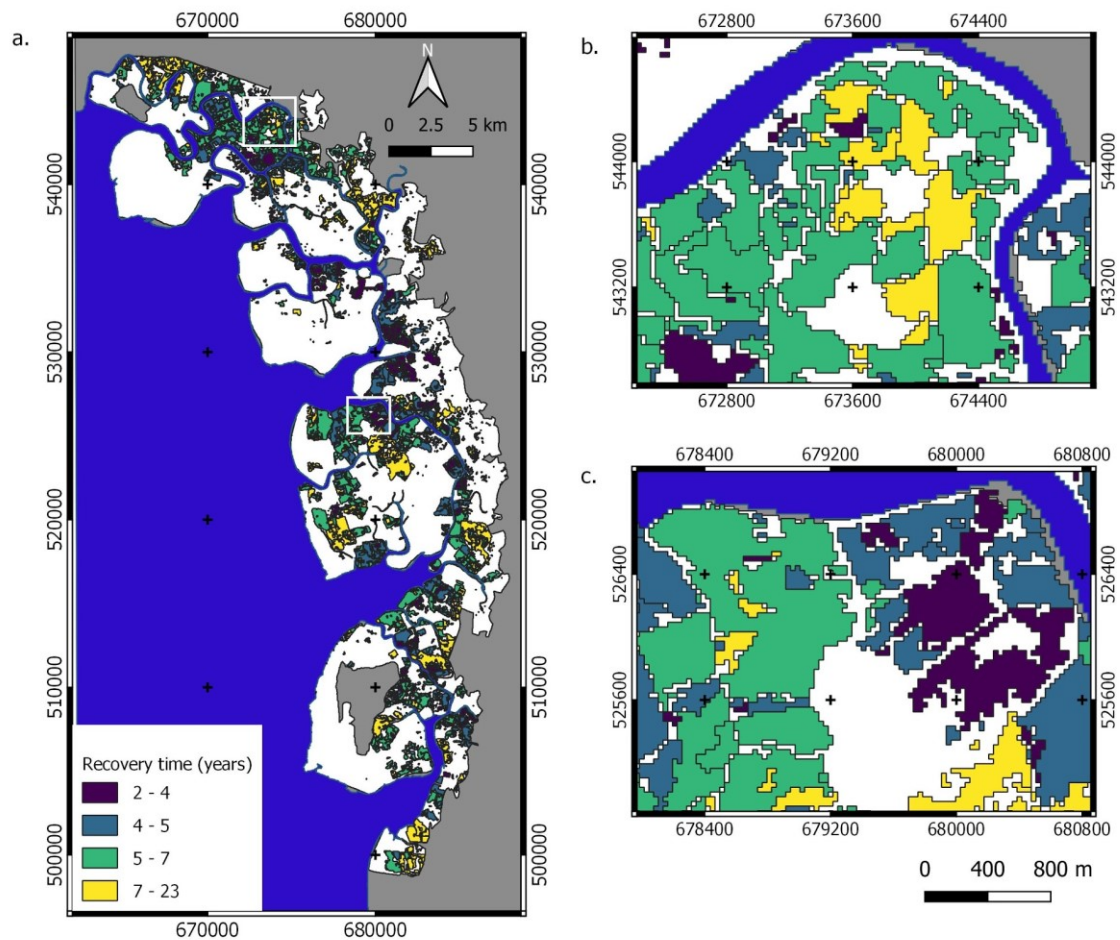


Figure 3. Map of the coupes that represent the areas of the forest that were clear felled in the same year (a). The black lines indicate the borders of each coupe. The colours indicate the recovery time per coupe grouped by quartiles. Two detailed views of the areas indicated with a white rectangle in the top (Figure 3b) and another white rectangle in the centre (Figure 3c) are shown. The grey areas are outside the reserve. The white areas indicate places where no clear-felling events were detected or areas that were clear-felled but did not completely recover by 2015.

The distance calculation to the closest forest stands and the closest water body is shown in Figure 4 and supplementary data S1 and S2. The closest forest stand could be a patch of dryland forest in the protective zones (supplementary material S2), or a *Rhizophora* stand in the productive, restrictive productive or protective zones (supplementary material S1).

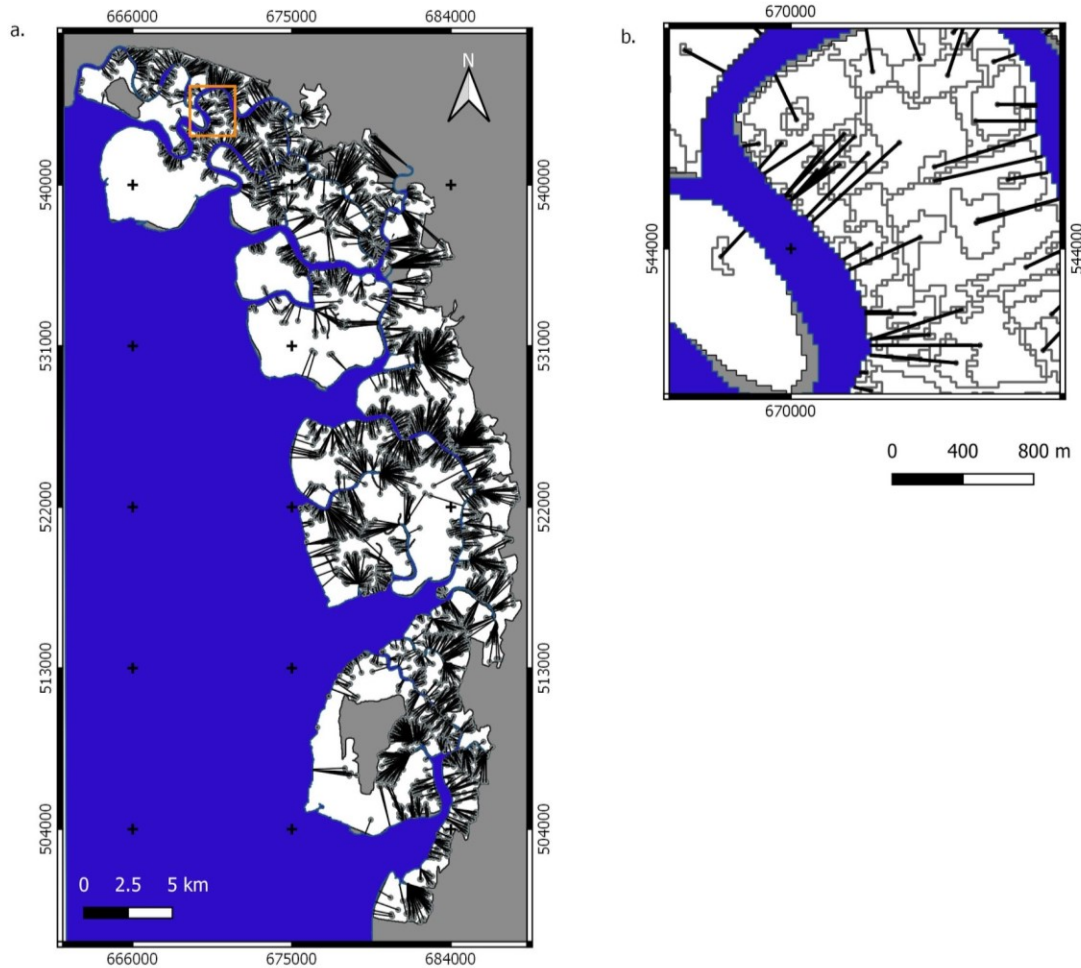


Figure 4. The distance calculation from the centres of each coupe to the closest water bodies indicated in blue. The black lines indicate the shortest distance to a water body, the points indicate the centre of each coupe and the grey lines the borders of the coupes. The grey areas are outside the reserve. (b) A detailed view is shown which correspond to the orange square indicated in Figure 4a. The area of the reserve is indicated in white.

3.2 Spatial context analysis

3.2.1 Univariate analysis

3.2.1.1 Univariate analysis for the recovery time

The average recovery time distribution was grouped in its corresponding four quartiles. Based on those four groups, the distances to the different types of land cover were analysed (supplementary data Figure S3, Table S2 and Table S3). Afterwards, we regrouped the quartiles into two new groups: the fast and the slow

recovery time. The fast group included the first, second and third quartile, meaning that, coupes that recovered between 2 and 6.86 years. The slow group corresponded to the fourth quartile, with these associated with coupes that recovered between 6.87 and 23 years. We compared the fast and slow groups to the distances to the *Rhizophora* stands, the dryland forest stands and to the water (Figure 5). A positive relationship with distance was observed in certain locations, with faster recoveries associated with coupes that were closer to water and *Rhizophora* stands (Figure 5a, 5c). It is noteworthy that the difference in distance to *Rhizophora* stands between fast and slow recovery coupes was relatively small (30 m and 33.5 m respectively). By contrast, coupes that were closer to dryland forest stands experienced slower recovery times (Figure 5b).

We further analysed the differences between the fast and the slow recovery groups. Based on the Wilcoxon Rank Sum Test, a statistically significant difference was observed at the 0.05 level between the fast and the slow group for the distance to water bodies, dryland forest stands and the nearest *Rhizophora* stand (see Figure 5).

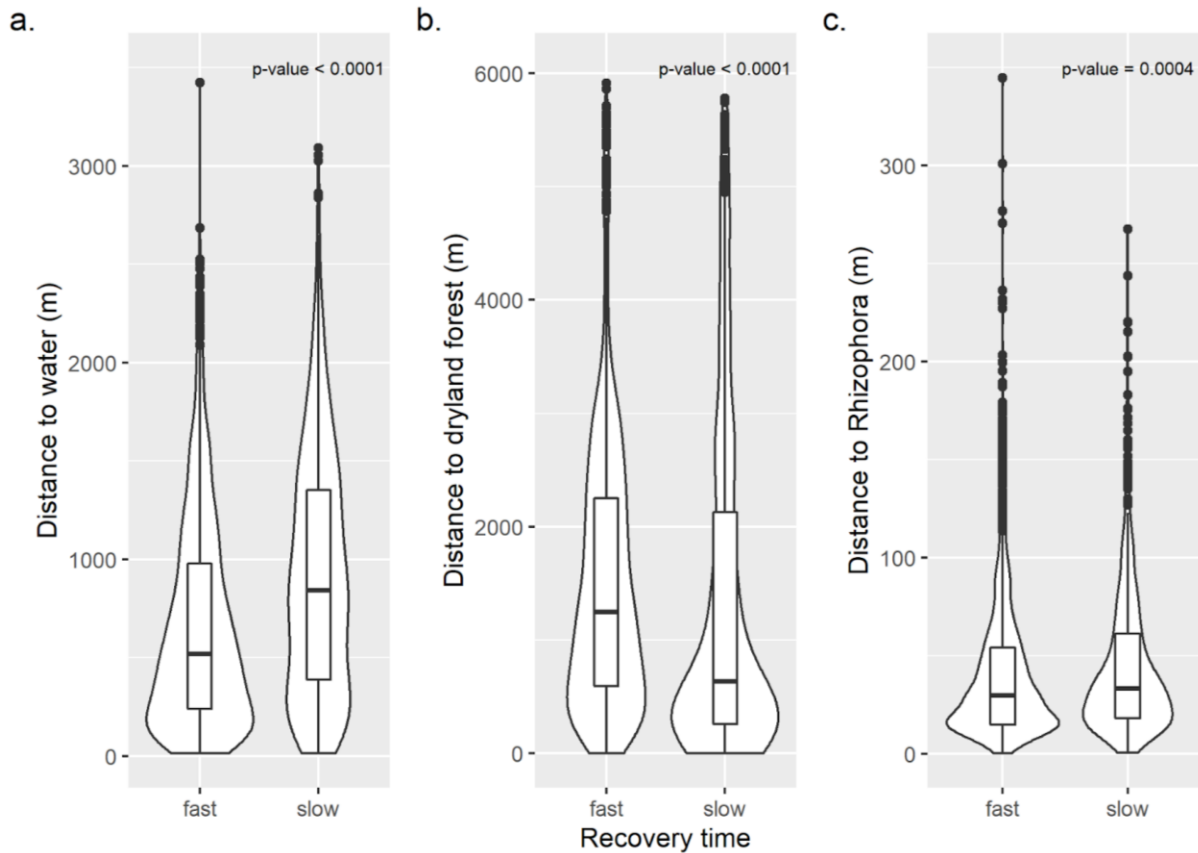


Figure 5. The box plots and the probability distribution of the recovery time groups. The relationship between the fast and slow recovery time groups and the distance to a) water bodies, b) dryland forest stands and c) *Rhizophora* stands (Figure 5c) are shown. The fast recovery time group are coupes that recovered between 2 and 6.9 years, and the slow recovery time group are coupes recovered between 6.9 and 23 years. The *p*-value is indicated for the comparison between the median distance of the fast and slow recovery time groups to the three different types of land cover.

3.2.1.2 Univariate analysis for the standard deviation of the recovery time

The standard deviation of the recovery time was analysed based on the four quartiles of its distribution (supplementary data Figure S4, Table S4 and Table S5). The median value of the standard deviation (interquartile range) of the recovery time was 0.8 (0.42 - 1.47), the minimum standard deviation value was zero and the maximum 8.5. We regrouped the quartiles into two new groups, with these experiencing low and high standard deviations of recovery times. The low group included the first, second and third quartile,

with these being coupes with a standard deviation of the recovery time between zero and 1.47. The high group corresponded to the fourth quartile, meaning that, coupes in which the standard deviation varied from 1.48 to 8.5. We compared the low and high standard deviation groups to the distances to *Rhizophora* stands, dryland forest stands and water (Figure 6). The coupes that were closer to water and *Rhizophora* stands had a lower standard deviation in the recovery time (Figure 6a, 6c). By contrast, the coupes that were closer to dryland forest stands had a higher standard deviation compared to the ones that are farther away (Figure 6b).

We further analysed the differences between the low and high standard deviation groups. Based on the Wilcoxon Rank Sum Test, there is a statistically significant difference at the 0.05 level between the low and high standard deviation groups for the distances to water bodies, dryland forest stands and closest *Rhizophora* stand (Figure 6).

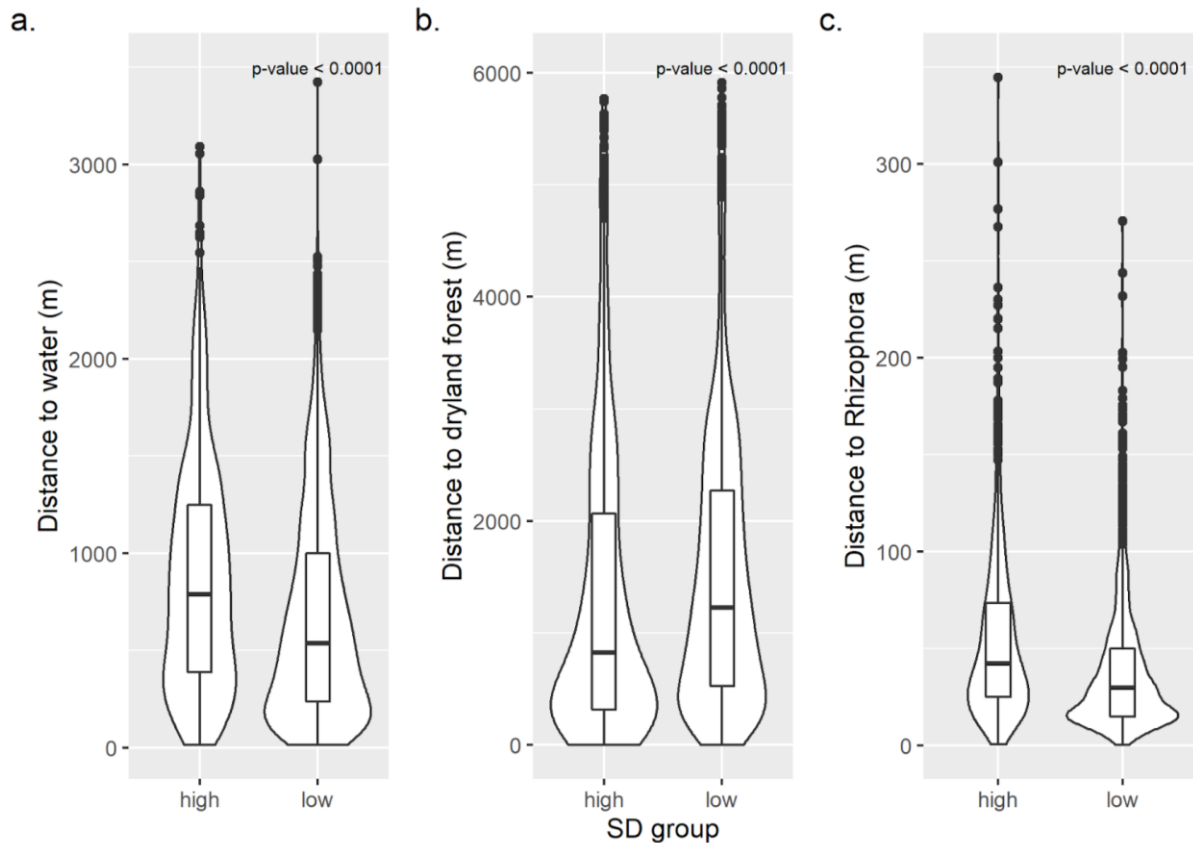


Figure 6. The box plots and the probability distribution of the standard deviation (SD) of the recovery time groups. The relationship between the high (1.48 to 8.5) and low (0 to 1.47) standard deviation of the recovery time groups and the distance to a) water bodies, b) dryland forest stands and c) *Rhizophora* stands are shown. The *p*-value is indicated for the comparison between the median distance of the high and low standard deviation of the recovery time groups to the three different types of land cover.

3.2.2 Multivariate analysis

3.2.2.1 Multivariate analysis of the average recovery time

The first GLS model was used to test the significance of each type of distance to explain the differences in the average recovery time per coupe. Based on the model, the distance to water bodies, dryland forests and *Rhizophora* stands contributed significantly to the changes in the average recovery time at the 0.05 level (Table 1). Coupes closer to water bodies and *Rhizophora* stands regenerated at a faster rate, whilst those closer to dryland forest stands were slower than those further away.

Table 1. GLS model results for the average recovery time. This model was corrected for spatial autocorrelation using a Gaussian structure (Adjusted R² Nagelkerke = 0.061).

Variable	Coefficient	<i>p</i> -value
Distance to water (km)	0.896 ± 0.073	<0.0001
Distance to dryland forest stands (km)	-0.066 ± 0.033	0.042
Distance to <i>Rhizophora</i> stands (km)	7.866 ± 1.127	<0.0001

3.2.2.2 Multivariate analysis of the standard deviation of the recovery time

The second GLS model was used to test the significance of each type of distance to explain the standard deviation of the recovery time per coupe. Based on the model, the distance to water bodies and *Rhizophora* stands contributed significantly to the changes in the standard deviation of the recovery time at the 0.05 level (Table 2). The closer a coupe was to water bodies or a *Rhizophora* stand, the lower the standard deviation in the recovery time per coupe. By contrast, the closer a coupe was to a dryland forest stand, the higher the standard deviation of the recovery time per coupe.

Table 2. GLS model results for the standard deviation of the recovery time. This model was corrected for spatial autocorrelation using a Gaussian structure (Adjusted R² Nagelkerke = 0.069).

Variable	Coefficient	<i>p</i> -value
Distance to water (km)	0.245 ± 0.053	<0.0001
Distance to dryland forest stands (km)	-0.034 ± 0.027	0.2027
Distance to <i>Rhizophora</i> stands (km)	6.497 ± 0.47	<0.0001

4. Discussion

4.1 Distance calculation

In this study we calculated the distances between the centres of areas that were clear-felled in the same year (*i.e.*, coupes) and three different types of land cover: water bodies, dryland forest stands and *Rhizophora* stands. Two important considerations were made in order to calculate these distances. (i) First, this study used coupes (*i.e.*, areas that were clear-felled in the same year) as the unit of analysis. We can rely in the information aggregated by coupes instead of pixels, as the average recovery time based on coupes is similar to the average recovery time using pixels as unit of analysis (5.6 ± 2.4 years based on coupes vs. 5.9 ± 2.7 years based on pixels) (Otero *et al.*, 2019). (ii) Second, the recovery time calculation was based on the NDMI, with this indicative of percentage canopy cover (Lucas *et al.*, 2019) Therefore, it is only describing the behaviour of the first years of regeneration as vegetation indices saturate in dense vegetation (Baret and Guyot, 1991, Huete *et al.*, 2002, Jackson *et al.*, 2004). Nevertheless, we are able to capture differences in the recovery time prior to the saturation of the index and establish a relationship between these differences and the distance to different types of land cover such as water bodies, dryland forest stands and *Rhizophora* stands.

4.2. Spatial context analysis

We found a relationship between proximity to (i) water bodies, (ii) dryland forest stands and (iii) *Rhizophora* stands and the average and standard deviation of the recovery time per coupe. (i) The closer a coupe is to water, the faster the regeneration compared to the coupes that are farther away. Mangrove propagules are dispersed by water (Tomlinson, 2016) and can be carried towards the edges of a water body by the direction of the water runoff (Di Nitto *et al.*, 2013, Sousa *et al.*, 2007). Therefore, propagules can more easily accumulate and therefore establish on areas that are closer to the borders of water bodies. This phenomena could also explain why the closer a coupe is to a water body, the lower the standard deviation of the recovery time within the coupe compared to those farther away. Although the propagules could also be washed away by tides, they can be trapped by vegetation and remain on land (Chang *et al.*, 2008, Di

Nitto et al., 2008, Di Nitto *et al.*, 2013), which seems to be the case in our study area. Hickey *et al.*, (2018) also observed the positive effect of the proximity to water in mangrove tree growth. They found that the closer a mangrove stand was to the water, the taller the trees compared to stands located further away from water bodies. As a result, higher estimates of biomass and carbon were observed in stands located closer to the water (Hickey *et al.*, 2018).

(ii) Coupes closer to dryland forest stands regenerated at a slower rate compared to those farther away. These forests are occasionally inundated by equinoctial tides and occur in more elevated soils on the landward side of the reserve (Ariffin and Mustafa, 2013, p. 30). Komiyama *et al.* (1996) and Sousa *et al.* (2007) reported lower establishment success of *Rhizophora* propagules at higher elevations due to higher soil hardness and difficulties for propagule rooting due to water standing in higher elevations. The topographic conditions in the dryland forests may not be suitable for establishment of *Rhizophora* propagules or these may be washed away by tides or freshwater discharge to lower elevation sites (Dahdouh-Guebas *et al.*, 2000, Di Nitto *et al.*, 2008, Di Nitto *et al.*, 2013, Sousa *et al.*, 2007). We also found that coupes closer to dryland forest stands have higher standard deviation in the recovery time within the coupe as compared to those farther away. Komiyama *et al.*, (1996) reported that even small changes in topography, such as 35 cm, have an impact on *Rhizophora* propagule establishment. Therefore, variations in elevation within a coupe could already have an impact on the spatial patterns of propagule establishment within a coupe (Di Nitto *et al.*, 2008, Sousa *et al.*, 2007).

(iii) Patch of *Rhizophora* trees were always able to be found close to every clear-felled area and therefore a natural supply of mangrove propagules is available (see supplementary material S1). The availability of propagules from adjacent mangrove stands is one of the key elements to ensure propagule dispersal (Bosire *et al.*, 2008, Di Nitto *et al.*, 2008). Moreover, we found that the standard deviation of the recovery time within a coupe is lower if that coupe is closer to a *Rhizophora* stand. *Rhizophora* propagules do not move by large distances from the parental tree, changing location from 2 to 20 m (Chan and Husin, 1985, Sousa

et al., 2007). The difference in the median distance from a *Rhizophora* stand for the coupes that recovered with a lower standard deviation as compared to the ones with higher standard deviation is 12 m. This small change in distance can explained the differences in the variability in recovery times within a coupe. Although mangrove propagules are hydrochorous and could potentially travel large distances, the average travel inside mature stands could be small (Sousa et al., 2007).

The relationships that we found between the recovery time and the proximity to different types of land cover based on the univariate analysis match the results obtained with the GLS models. The proximity to water and *Rhizophora* stands has a positive relationship with the recovery time between and within coupes. By contrast, proximity to dryland forest stands has a negative relationship with the recovery time between and within coupe. However, the explanatory power of the GLS models is very low. These models are only considering the proximity to different types of land cover to explain the recovery time. However, propagule dispersal and establishment are influenced by additional factors such as wind, currents, propagule predation, geomorphology, nutrient availability and salinity (Di Nitto et al., 2008, Di Nitto et al., 2013, Komiyama et al., 1996, Sousa et al., 2007; Tomlinson, 2016; Van der Stocken et al., 2015, Van Nederveelde et al, 2015). Though more studies are needed to further explain the influence of these factors on the variations of the recovery time, this study can guide the definition of new research questions and planning of new field studies that contribute to the understanding of the changes in the recovery patterns in the MMFR.

4.3. Implication for the local management

We found a relationship between the recovery time and the distance to different types of land cover. These insights about the regeneration of mangrove forests in the MMFR could guide future strategies implemented by the local management (e.g., evaluating the current replantation policy of the reserve). An option is to link the areas that required replanting with the coupes identified in this study and analyse if there is an effect of replantation of propagules in the recovery time. Also, future decisions on the distribution of productive

and protective zones in the reserve can be guided by this research (*e.g.* by taking into account the proximity to water and dryland forest stands to ensure a proper regeneration of mangrove stands after clear-felling).

We found clear-felling events in 18 % of the area indicated to be dryland forest stands and 12 % in the area of *Rhizophora* protective stands. We digitized and georeferenced the map that describes the protective zones available in the management plan from 2010 to 2019 to create the digital version of the map of the protective zones. According to the local management, maps are updated for each management plan. For the last management plan (2010 to 2019), a mosaic of two Satellite Pour l'Observation de la Terre (SPOT) images from 2007 and 2009 was used to update changes in the distribution of river channels, new infrastructure, erosion, accretion, and boundaries of *Avicennia*, *Sonneratia* and dryland forest stands (Ariffin and Mustafa, 2013, p. 33). However, we used Landsat annual time series from 1988 to 2015 to detect the clear-felling events and calculate the recovery time (Otero *et al.*, 2019) and consider that time-series optical (Otero *et al.*, 2019) and radar data (Lucas *et al.*, 2019) can be used to provide new information on the changes in the reserve that cannot be captured by using a single image. Additionally, the changes that we observed in protective areas could be an indication that the current management plan maps require a more detailed update in certain areas. Moreover, the last management plan reported the species composition of the dryland forest stands based on the study by Chan (1989). We suggest that a reassessment of the current forest structure of the dryland forests is necessary, as well as a study of the topography of the MMFR.

5. Conclusions

In this study we were able to identify the relationship between the recovery time of different coupes and the proximity to different types of land cover. We found a positive relationship with proximity to water and *Rhizophora* stands, meaning that, the closer a coupe is to a water body or *Rhizophora* stand, the faster it recovered from a clear-felling event as compared to coupes that are farther away. By contrast, there is a negative relationship between the proximity to dryland forest stands and the recovery time. These results can be used by the local management to evaluate the current replantation policy, to guide monitoring

activities in protective and productive zones, and to guide decisions on the distribution of the areas to be clear-felled in the future. This study recommends that satellite sensor data be more widely considered for mapping and monitoring the past and current dynamics of mangroves in the MMFR to assist management.

Funding: This research was funded by BELSPO (Belgian Science Policy Office) in the frame of the STEREO III Programme — Project Managing Mangrove Forests with Optical and Radar Environmental Satellites (MAMAFORST) grant number SR/00/323. The European Regional Development Fund (ERDF) Ser Cymru program is also thanked for funding Prof. Lucas.

Acknowledgments: We would like to thank the Perak State Forestry Department and the local rangers of the MMFR for their support during the fieldwork and for providing the management plans of the reserve. This study was carried out with the approval of the Perak State Forestry Department, Ipoh, Malaysia.

Conflicts of interest

Conflicts of interest: none

References

- Allen, C.R, Angeler, D.G., Cumming, G.S., Folke, C., Twidwell, D. and Uden D.R. (2016) Quantifying spatial resilience. *Journal of Applied Ecology* 53, 625 - 635.
- Alongi, D.M. Carbon sequestration in mangrove forests. *Carbon Management* 2012, 3, 313-322.
- Alongi, D.M. Mangrove forests: Resilience, protection from tsunamis, and responses to global climate change. *Estuarine, Coastal and Shelf Science* 2008, 76, 1 -13.
- Alongi, D. M. Present state and future of the world's mangrove forests. *Environmental Conservation* 29 (3), 331 - 349.
- Amir, A.A. (2012). Canopy gaps and the natural regeneration of Matang mangroves. *Forest Ecology and Management* 269, 60-67. <https://doi.org/10.1016/j.foreco.2011.12.040>

497 Ariffin, R. and Mustafa N.M.S.N. (2013). A Working Plan for the Matang Mangrove Forest Reserve, Perak (6th
 498 revision). Malaysia: State Forestry Department of Perak.

499 Aslan, A., Rahman, A.F. Warren, M.W. and Robeson, S.M. (2016). Mapping spatial distribution and biomass of
 500 coastal wetland vegetation in Indonesian Papua by combining active and passive remotely sensed data. *Remote*
 501 *Sensing of Environment* 183, 65-81. <https://doi.org/10.1016/j.rse.2016.04.026>

502 Asthon, E.C., Hogart, P.J. and Ormond, R. "Breakdown of mangrove leaf litter in a managed mangrove forest in
 503 Peninsular Malaysia". *Hydrobiologia*, vol. 413, pp. 77 - 88, 1999.

504 Azahar M, Nik Mohd Shah NM (2003). A Working Plan for the Matang Mangrove Forest Reserve, Perak: the third
 505 10- year period (2000–2009) of the second rotation (5th revision). Malaysia: State Forestry Department of Perak.

506 Aziz, A.A., Pinn, S. and Dargusch, P. (2015). Investigating the decline of ecosystem services in a production mangrove
 507 forest using Landsat and object-based image analysis. *Estuarine, Coastal and Shelf Science* 164, 353 – 366.
 508 <https://doi.org/10.1016/j.ecss.2015.07.047>

509 Aziz, A.A., Thomas, S., Dargusch, P. and Phinn, S. (2016). Assessing the potential of REDD+ in a production
 510 mangrove forest in Malaysia using stakeholder analysis and ecosystem services mapping. *MARine Policy* 74, 6-17.
 511 <https://doi.org/10.1016/j.marpol.2016.09.013>

512 Baret, F. and Guyot, G. Potential and limits of vegetation indices for LAI and APAR Assessment. *Remote Sensing of*
 513 *Environment* 1991, 35, 161 – 173.

514 Bosire, J.O., Dahdouh-Guebas, F., Walton, M., Crona, B.I., Lewis III., R.R., Field. C., Kairo, J.G. and Koedam, N.
 515 Functionality of restored mangroves: A review. *Aquatic Botany* 2008, 89, pp. 251 - 259.

516 Bunting, P., Rosenqvist, A., Lucas. R.M., Rebelo, L, Hilarides, L. Thomas, N., Hardy, A., Itoh, T., Shimada, M. and
 517 Finlayson, C.M. (2018). The Global Mangrove Watch - A New 2010 Global Baseline of Mangrove Extent. *Remote*
 518 *Sensing* 10 (10), 1669. doi:10.3390/rs10101669

519 Camarretta, N., Puletti, N., Chiavetta, U. and Corona, P. (2017). Quantitative changes of forest landscapes over the
 520 last century across Italy. *Plant Biosystems* 152 (5), 1011-1019.

521 Chan, H. T., and N. Husin. 1985. Propagule dispersal, establishment, and survival of *Rhizophora mucronata*. *The*
 522 *Malaysian Forester* 48:324–329.

523 Chang, E. R., Veeneklaas, R. M., Buitenwerf, R., Bakker, J. P., and Bouma, T. J. (2008). To move or not to move:
 524 determinants of seed retention in a tidal marsh, *Funct. Ecol.*, 22, 720–727.

525 Chan, H.T. (1989). A note on tree species productivity of a natural dryland mangrove forest in Matang, Peninsular
526 Malaysia. *Journal Tropical Forest Science* 1(4), 399 - 400.

527 Chong, V.C. (2006). Sustainable utilization and management of mangrove ecosystems of Malaysia. *Aquatic*
528 *Ecosystems Health and Management* 9 (2), 249 - 260.

529 Cliff, A.D. and Ord, K. (1970). Spatial autocorrelation: a review of existing and new measures with applications.
530 *Economic Geography* 46, 269 - 292.

531 Conchedda, G., Durieux, L. and Mayaux, P. (2008). An object-based method for mapping and change analysis in
532 mangrove ecosystems. *ISPRS Journal of Photogrammetry and Remote Sensing*
533 63 (5), 578-589. <https://doi.org/10.1016/j.isprsjprs.2008.04.002>

534 Crawley, M.J. (2007). *The R book*. John Wiley & Sons Ltd, England.

535 Dahdouh-Guebas, F., A. Verheyden, W. De Genst, S. Hettiarachchi & N. Koedam (2000). Four decade vegetation
536 dynamics in Sri Lankan mangroves as detected from sequential aerial photography : a case study in Galle. *Bulletin*
537 *of Marine Science* 67(2): 741-759.

538 Di Nitto, D., Dahdouh-Guebas, F., Kairo, J.G., Decleir, H. and Koedam, N. (2008). Digital terrain modelling to
539 investigate the effects of sea level rise on mangrove propagule establishment. *Marine Ecology Progress Series* 356,
540 175-188. doi: 10.3354/meps07228

541 Di Nitto, D., Erfemeijer, P. L. A., van Beek, J. K. L., Dahdouh-Guebas, F., Higazi, L., Quisthoudt, K., Jayatissa, L.
542 P., and Koedam, N. (2013). Modelling drivers of mangrove propagule dispersal and restoration of abandoned shrimp
543 farms. *Biogeosciences* 10, 5095–5113.

544 Donato, D.C., Kauffman, J.B., Murdiyarso, D., Kurnianto, S., Stidham, M. and Kanninen, M. Mangroves among the
545 most carbon-rich forest in the tropics. *Nature Geoscience* 2011, vol., 4, pp. 293 - 297.

546 Duke, N.C., Ball, M.C. and Ellison J.C. Factors influencing biodiversity and distributional gradients in mangroves.
547 *Global Ecology and Biogeography Letters* 1998, vol. 7, pp. 27 - 47.

548 Ellison, A. Mangrove restoration: do we know enough?. *Restoration Ecology* 2000, vol. 8, pp. 219 - 229.

549 FAO. 2007. The World's Mangroves 1980-2005. FAO Forestry Paper 153, Food and Agriculture Organization, Rome.

550 Feller, I.C., Friess, D.A., Krauss, K.W. and Lewis III, R. R. (2017). The state of the world's mangroves in the 21st
551 century under climate change. *Hydrobiologia* 803, 1 - 12. DOI 10.1007/s10750-017-3331-z

552 Goessens, A., Satyanarayana, B., Van der Stocken, T., Quispe Zuniga, M., Moh-Lokman, H., Sulong, I. and Dahdouh-

553 Guebas, F. (2014). Is Matang Mangrove Forest in Malaysia sustainably rejuvenating after more than a century of
 554 conservation and harvesting management? PLoS ONE 9 (8).

555 Gong W.K. and Ong J.E. (1995). The use of demographic studies in mangrove silviculture. *Hydrobiologia* 195, 255 -
 556 261.

557 Hamunyela, E. Verbesselt, J. and Herold, M. (2016). Using spatial context to improve early detection of deforestation
 558 from Landsat time series. *Remote Sensing of Environment* 172, 126-138. <https://doi.org/10.1016/j.rse.2015.11.006>

559 Herold, M., Couclelis, H. and Clarke, K.C. (2005). The role of spatial metrics in the analysis and modeling of urban
 560 land use change. *Computers, Environment and Urban Systems* 29, 369 - 399.

561 Hickey, S.M., Callow, N.J., Phinn, S., Lovelock, C.E. and Duarte, C.M. (2018). Spatial complexities in aboveground
 562 carbon stocks of a semi-arid mangrove community: A remote sensing height-biomass-carbon approach. *Estuarine,
 563 Coastal and Shelf Science* 200, 194-201. <https://doi.org/10.1016/j.ecss.2017.11.004>

564 Huete, A., Didan, K., Miura, T., Rodriguez, E.P., Gao, X. and Ferreira, L.G. Overview of the radiometric and
 565 biophysical performance of the MODIS vegetation indices. *Remote Sensing of Environment* 2002, 83, 195-213.
 566 [https://doi.org/10.1016/S0034-4257\(02\)00096-2](https://doi.org/10.1016/S0034-4257(02)00096-2)

567 Jackson, T.J., Che, D., Cosh, M., Li, F., Anderson, M., Walthall, C., Doriaswamy, P. and Hunt E.R. Vegetation water
 568 content mapping using Landsat data derived normalized difference water index for corn and soybeans. *Remote Sensing
 569 of Environment* 2004, 92, 475 – 482.

570 Kairo, J.G., Dahdouh-Guebas, F., Bosire, J. and Koedam, N. (2001). Restoration and management of mangrove
 571 systems - a lesson for and from the East African region. *South African Journal of botany*, 67, 383-389.

572 Kock, E.W., Barbier, E.B., Silliman, B.R., Reed, D.J., Perillo, G.E, Hacker, S.A. et al. (2009). Non-linearity in
 573 ecosystem services: temporal and spatial variability in coastal protection. *Front Ecol Environ* 7(1), 29–37.
 574 doi:10.1890/080126

575 Komiyama, A., Santian, T., Higo, M., Patanaponpaiboon, P., Kongsangchai J., and Ogino K. (1996).
 576 Microtopography, soil hardness and survival of mangrove (*Rhizophora apiculata* BL.) seedlings planted in an
 577 abandoned tin-mining area. *Forest Ecology and Management* 81, 243 - 248.

578 Lewis III, (2005). Ecological engineering for successful management and restoration of mangrove forests. *Ecological
 579 Engineering* 24, (4), 403-418. <https://doi.org/10.1016/j.ecoleng.2004.10.003>

580 López-Portillo, J. Lewis III, R.R. Saenger, P., Rovai, A., Koedam, N., Dahdouh-Guebas, F., Agraz-Hernández, C. and
 581 Rivera-Monroy, V.H. (2017). Mangrove Forest Restoration and Rehabilitation. In Rivera-Monroy *et al.* (eds.),
 582 Mangrove Ecosystems: A Global biogeographic Perspective. Springer International Publishing. pp. 301-345.
 583 https://doi.org/10.1007/978-3-319-62206-4_10.
 584 Lucas, R.M., Van De Kerchove, R., Otero, V., Lagomasino, D., Fatoyinbo, L., Satyanarayana, B. and Dahdouh-
 585 Guebas, F. (2019). New Insights into the Structural Composition of Mangroves Achieved Through Combining
 586 Multiple Sources of Remote Sensing Data. Remote Sensing of Environment (in review)
 587 Magee, L. (1990). R^2 measures based on Wald and Likelihood Ratio Joint Significance Tests. The American
 588 Statistician 44(3), 250-253.
 589 Mukherjee, N., Sutherland, W.J. Khan, M.N.I. Berger, U. Schmitz, N. Dahdouh-Guebas, F. and Koedam, N. (2014).
 590 Using expert knowledge and modeling to define mangrove composition, functioning, and threats and estimate time
 591 frame of recovery. *Ecol. Evol* vol 4, 2247–2262.
 592 Nagelkerke, N.J.D. (1991). A Note on a General Definition of the Coefficient of Determination. *Biometrika*, 78 (3),
 593 691-692.
 594 Otero, V., Van De Kerchove, R., Satyanarayana, B., Mohd-Lokman, H., Lucas, R. and Dahdouh-Guebas, F. (2019).
 595 An Analysis of the Early Regeneration of Mangrove Forests using Landsat Time Series in the Matang Mangrove
 596 Forest Reserve, Peninsular Malaysia. *Remote Sensing* 11 (7), 774. <https://doi.org/10.3390/rs11070774>
 597 Peng, Y., Diao, J., Zheng, M., Guan, D., Zhang, R., Chen, G. and Lee S.Y. (2016). Early growth adaptability of four
 598 mangrove species under the canopy of an introduced mangrove plantation: Implications for restoration. *Forest Ecology*
 599 *and Management* 373, 179 - 188. <https://doi.org/10.1016/j.foreco.2016.04.044>
 600 Putz, F.E. and Chan, H.T. (1986). Tree growth, dynamics, and productivity in a mature mangrove forest in Malaysia.
 601 *Forest Ecology and Management* 17, 211 – 230.
 602 QGIS Development Team (2018). QGIS Geographic Information System version 3.4.4 Madeira. Open Source
 603 Geospatial Foundation Project. <http://qgis.osgeo.org>
 604 Ribeiro, M.C., Metzger, J.P., Camargo Martensen, A., Ponzoni, F.J. and Hirota, M.M. (2009). The Brazilian Atlantic
 605 Forest: How much is left, and how is the remaining forest distributed? Implications for conservation. *Biological*
 606 *Conservation* 142, 1141-1153. doi:10.1016/j.biocon.2009.02.021
 607 Rivera-Monroy, V.H., Twilley, R.R., Medina, E. et al. *Estuaries* (2004). Spatial variability of soil nutrients in disturbed

riverine mangrove forests at different stages of regeneration in the San Juan River estuary, Venezuela. *Estuaries* 27(10), 44-57. <https://doi.org/10.1007/BF02803559>

RStudio Team (2016). RStudio: Integrated Development for R. RStudio, Inc., Boston, USA, <http://www.rstudio.com>

Saenger, P. (2002). Mangrove Ecology, Silviculture and Conservation. Kluwer Academic Publishers, Dordrecht, The Netherlands, p. 229-243.

Sillanpaa, M., Vantellingen, J. and Friess, D.A. (2017). Vegetation regeneration in a sustainably harvested mangrove forest in West Papua, Indonesia. *Forest Ecology and Management* 390, 137 - 146.

Simard, M., Fatoyinbo, L., Smetanka, C., Rivera-Monroy, V.H., Castañeda-Moya, E., Thomas, N. and Van der Stocken, T. (2019). Mangrove canopy height globally related to precipitation, temperature and cyclone frequency. *Nature Geoscience* 12, 40-45.

Sousa, W.P., Kennedy, P.G. and Mitchell, B.J. (2003) Propagule size and predispersal damage by insects affect establishment and early growth of mangrove seedlings. *Oecologia* 135, 564 - 575.

Sousa, W.P, Kennedy, P.G., Mitchell, B.J., and Ordonez, B. M. (2007) Supply-side Ecology In Mangroves: Do Propagule Dispersal And Seedling Establishment Explain Forest Structure? *Ecological Monographs* 77(1), 53–76.

Suyadi,, Gao, J., Lundquist, C.J. and Schwendenmann, L. (2018). Characterizing landscape patterns in changing mangrove ecosystems at high latitudes using spatial metrics. *Estuarine, Coastal and Shelf Science* 215, 1 - 10.

Tomlinson, P.B. *The botany of mangroves*. 2nd edition, Cambridge University Press, UK, 2016. pp. 135 - 136.

Van der Stocken, T., Vanschoenwinkel, B., De Ryck, D.J.R., Bouma, T.J., Dahdouh-Guebas, F., Koedam, N. Interaction between Water and Wind as a Driver of Passive Dispersal in Mangroves. *PLoS ONE* 2015, 10(3): e0121593. [doi:10.1371/journal.pone.0121593](https://doi.org/10.1371/journal.pone.0121593)

Van Nedervelde, F., Cannicci, S., Koedam, N., Bosire, J. and Dahdouh-Guebas, F. What regulates crab predation on mangrove propagules? *Acta Oecologica* 2015, 63, 63 - 70.

Walters, B.B., Rönnbäck, P., Kovacs, J.M., Crona, B., Hussain, S.A., Badola, R., Primavera, J.H., Barbier, E. and Dahdouh-Guebas, F. (2008). Ethnobiology, socio-economics and management of mangrove forest: A review. *Aquatic Botany*, 220 – 236.

Supplementary data Spatial Analysis

Table S1. Species composition of the dryland forests based on Chan (1989). Taken from the management plan from 2010 to 2019 (Ariffin and Mustafa, 2013). Trees indicated with * are mangroves major and minor components according to Tomlinson (2016).

Species	Density (trees/ha)
<i>Rhizophora apiculata</i> *	141
<i>Heritiera littoralis</i> *	130
<i>Ficus Microcarpa</i>	123
<i>Flacourtia jangomas</i>	77
<i>Oncosperma tigillarium</i>	71
<i>Bruguiera gymnorhiza</i> *	67
<i>Teijsmanniodendron holrungi</i>	53
<i>Barringtonia aisatica</i>	49
<i>Ilex cymosa</i>	31
<i>Planchonella obovata</i>	28
<i>Petunga roxburghii</i>	24
<i>Intsia bijuga</i>	19
<i>Euodia roxburghii</i>	18
<i>Canthium didymus</i>	16
<i>Polylthia sclerophylla</i>	9.8
<i>Cynometra ramiflora</i>	8
<i>Terenna fragans</i>	7.6
<i>Ardisia elliptica</i>	4.9
<i>Pittosporus ferrugineum</i>	3.6
<i>Ficus sundaica</i>	2.2
<i>Glochidion perakensis</i>	1.8

<i>Vitex pinnata</i>	1.8
<i>Eugenia kunstleri</i>	1.8
<i>Eugenia leuylon</i>	1.3
<i>Ficus annulata</i>	0.9
<i>Polyalthia glauca</i>	0.9
<i>Ficus obscura</i>	0.9
<i>Ficus bracteata</i>	0.4
<i>Xylocarpus granatum</i> *	0.4
<i>Ficus crassiramea</i>	0.4

5
6
7
8
9
10
11
12
13
14
15
16
17
18
19
20
21

Figure S1. Distance calculations from the centre points to *Rhizophora* stands

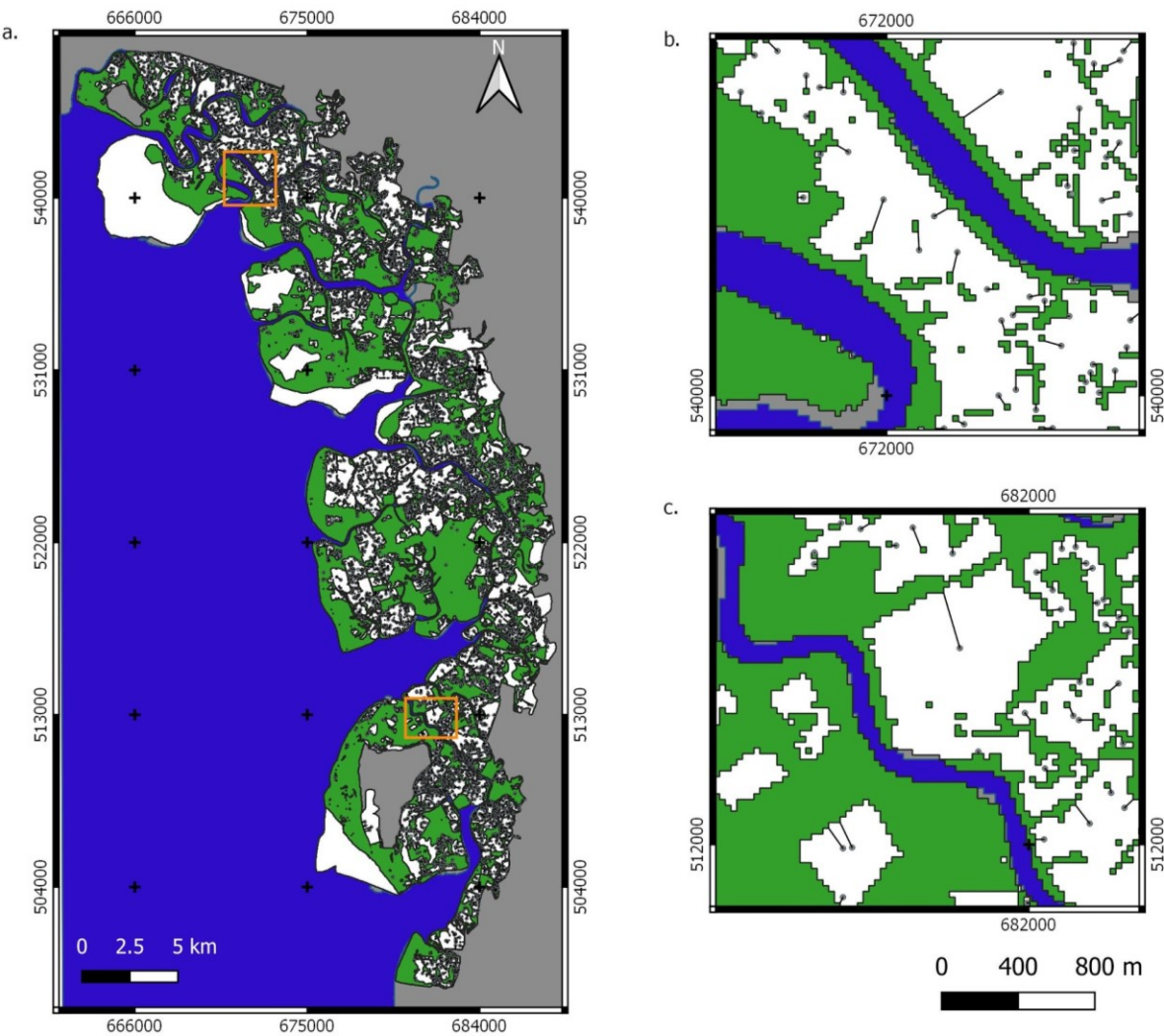
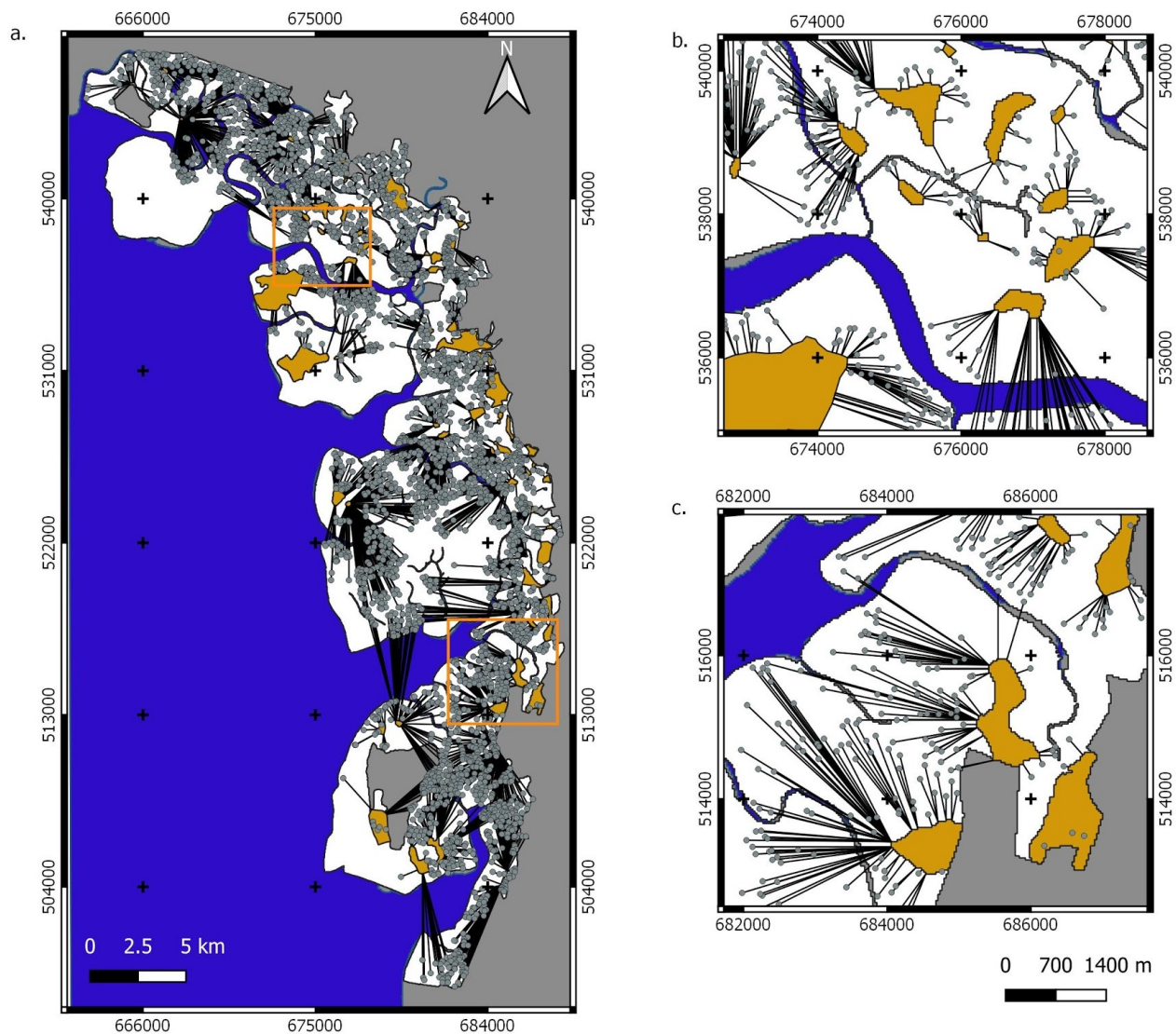


Figure S1. The distance calculations from the centre of the coupes to the closest *Rhizophora* stands (green areas). Two detailed areas are shown, (Figure S1b) indicated with an orange square in the top of Figure S1a, and (Figure S1c) indicated with an orange square on the bottom of Figure S1a. The white areas indicate places inside the reserve that were clear-felled between 1989 and 2015 or that are composed of another mangrove species such as *Avicennia* or *Sonneratia*. The grey areas are outside the reserve.

32 **Figure S2. Distance calculations from the centre points to dryland forest stands**



33
34 **Figure S2.** The calculation from the centre of the coupes to the closest dryland forest (orange areas). Two
35 detailed areas are shown, (Figure S2b) indicated with an orange square in the top of Figure S1a, and
36 (Figure S1c) indicated with an orange square on the left side of Figure S1a. The area of the reserve is
37 indicated in white, the grey areas are outside the reserve.

Figure S3. Analyses of the four quartiles of the average recovery time distribution according to the distance to water bodies, dryland forest stands and *Rhizophora* stands.

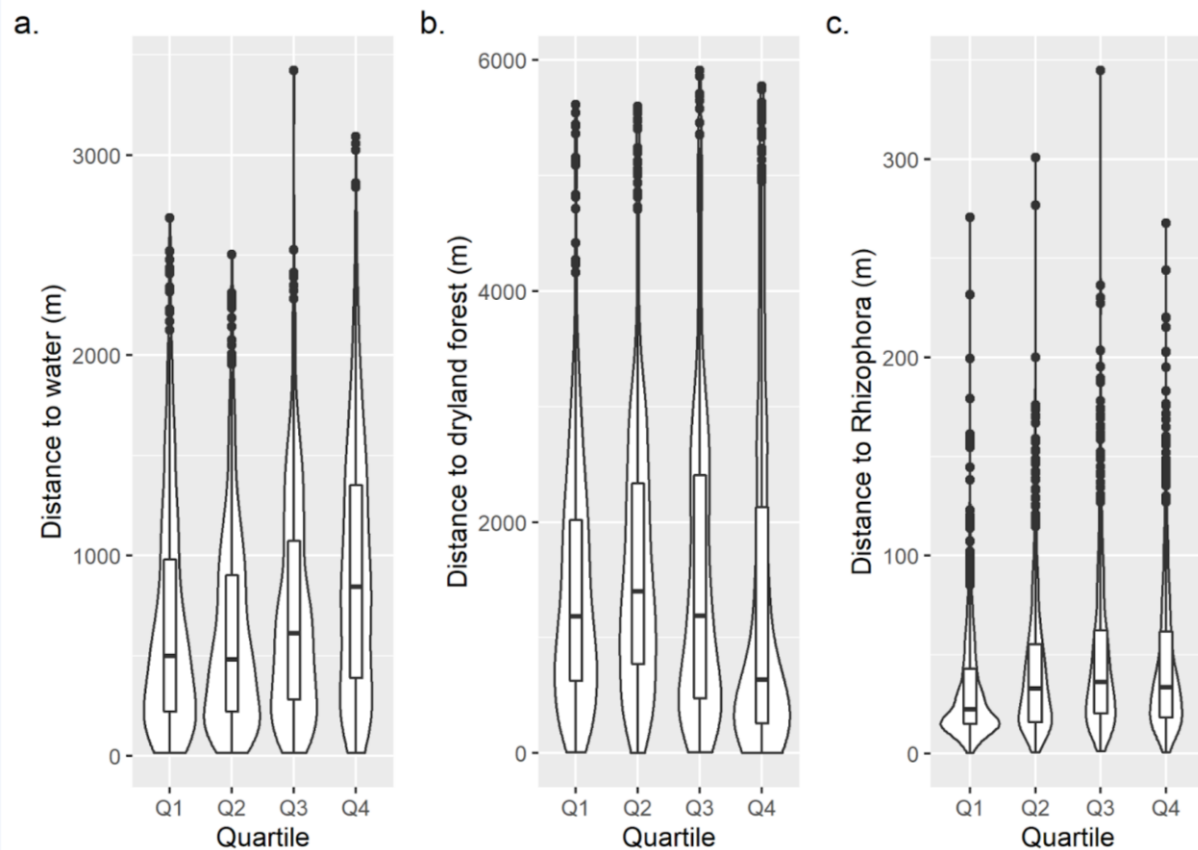


Figure S3. The box plots and the probability distribution of the recovery time quartiles. The relationship between the first (Q1), the second (Q2), the third (Q3) and the fourth (Q4) quartiles and the distance to a) water bodies, b) dryland forest stands and c) *Rhizophora* stands is shown. The first quartile include the coupes that recovered between 2 and 4.18 years, the second between 4.19 and 5.21 years, the third between 5.22 and 6.86 years, and the fourth between 6.87 and 23 years.

Table S2. Comparison between the quartiles of the average recovery time distribution and the distances to different types of forest and to the water. The first quartile is indicated as Q1, the second as Q2, the third as Q3 and the fourth as Q4. We used a Wilcoxon Rank Sum Test as each quartile did not have a normal distribution for each type of distance (Shapiro-Wilk test, p -value<0.0001)

Distance	Q1 and Q2	Q2 and Q3	Q3 and Q4
To water bodies	p -value=0.4676	p -value=0.0001	p -value<0.0001
To dryland forest stands	p -value<0.0001	p -value<0.0012	p -value<0.0001
To <i>Rhizophora</i> stands	p -value<0.0001	p -value=0.0068	p -value=0.2478

Table S3. Median distance (m) of each quartile of the recovery time distribution for each type of distance. The first quartile is indicated as Q1, the second as Q2, the third as Q3 and the fourth as Q4.

Distance	Median Q1	Median Q2	Median Q3	Median Q4
To water bodies	499.07	482.25	611.98	843.43
To dryland forest stands	1,183.92	1,398.66	1,190.06	635.84
To <i>Rhizophora</i> stands	22.5	33	36.18	33.54

Figure S4. Analyses of the standard deviation of the recovery time distribution according to the distance to water bodies, to dryland forest stands and *Rhizophora* stands

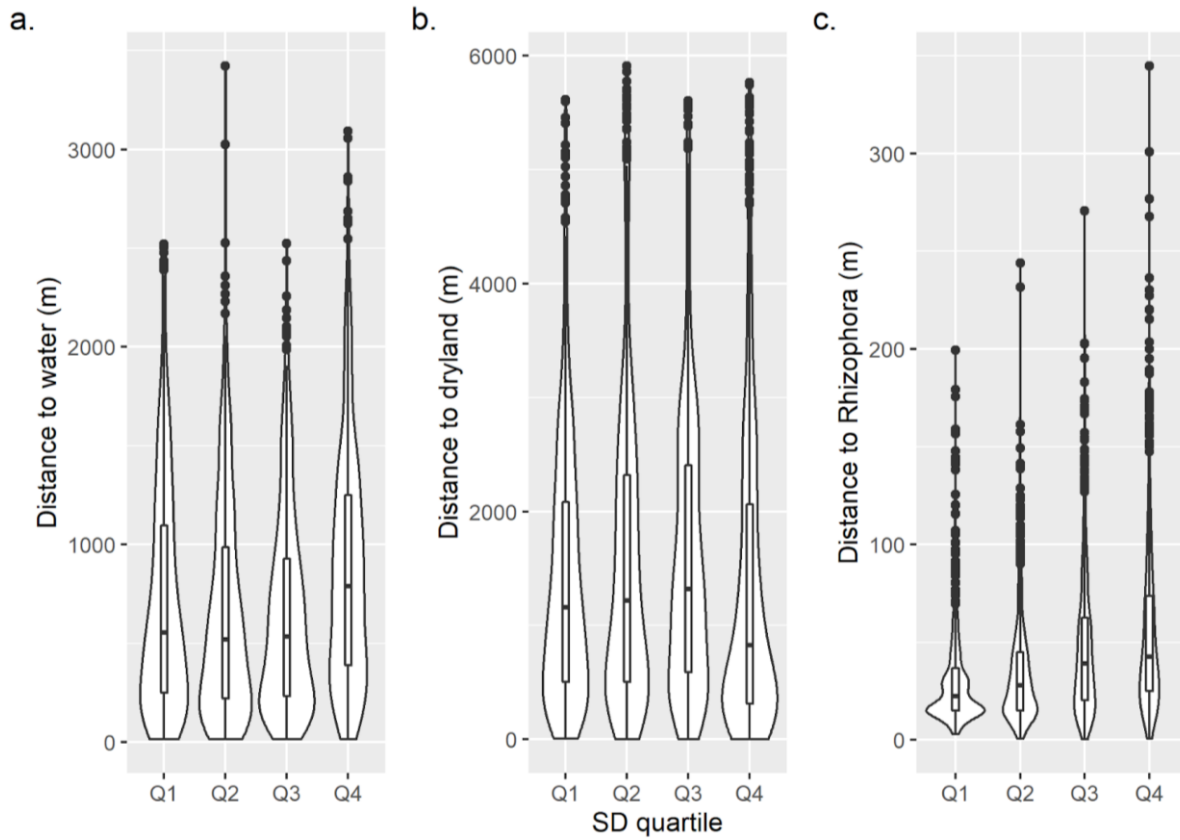


Figure S4. The box plots and the probability distribution of the standard deviation of the recovery time quartiles. The relationship between the first (Q1), the second (Q2), the third (Q3) and the fourth (Q4) quartiles and the distance to a) water bodies, b) dryland forest stands and c) *Rhizophora* stands is shown. The first quartile include the coupes that have a standard deviation between zero and 0.42, the second between 0.43 and 0.8, the third between 0.81 and 1.47, and the fourth between 1.48 and 8.5.

Table S4. Comparison between the quartiles of the standard deviation of the recovery time distribution and the distances to different types of forest and to the water. The first quartile is indicated as Q1, the second as Q2, the third as Q3 and the fourth as Q4. We used a Wilcoxon Rank Sum Test as each quartile did not have a normal distribution for each type of distance (Shapiro-Wilk test, p -value<0,0001)

Distance	Q1 and Q2	Q2 and Q3	Q3 and Q4
To water bodies	p -value=0.0571	p -value=0.6149	p -value<0.0001
To dryland forest stands	p -value=0.1777	p -value=0.1993	p -value<0.0001
To <i>Rhizophora</i> stands	p -value=0.0003	p -value<0.0001	p -value=0.0004

Table S5. Standard deviation of each quartile of the recovery time distribution for each type of distance. The first quartile is indicated as Q1, the second as Q2, the third as Q3 and the fourth as Q4.

Distance	Median Q1	Median Q2	Median Q3	Median Q4
To water bodies	553.17	518.17	532.66	789.53
To dryland forest stands	1,159.51	1,218.08	1,319.24	824.56
To <i>Rhizophora</i> stands	22.5	27.86	38.97	42.49